

Stability of MHD Unsteady Nanofluid Flow Through Expanding or Contracting Channel with Porous Walls

M. K. Rahman¹

¹Department of Mathematics, N.S. Govt. College, Natore, Bangladesh

Md. S. Alam^{2,*}

²Department of Mathematics, Jagannath University, Dhaka-1100, Bangladesh

M. A. H. Khan³

³Department of Mathematics, Bangladesh University of Engineering and Technology
Dhaka-1000, Bangladesh

Received 7 December 2016; Received in revised form 21 February 2017

Accepted 31 March 2017; Available online 12 October 2017

ABSTRACT

The objective of the present study is to investigate the influence of external magnetic field on unsteady incompressible flow of water based nanofluid through a successively expanding or contracting channel with porous walls. The basic governing equations with boundary conditions are non-dimensionalized using appropriate transformation to ordinary differential equations, which are then solved using power series with the help of Hermite-Padé approximation method. The instability of the flow is shown using bifurcation graph and the dominating singularity behavior numerically. The regular effects of the different governing physical parameters specifically Hartmann number, volume fraction of nanoparticles, non-dimensional shear stress and permeation Reynolds number on velocity profiles are depicted graphically.

Keywords: Expanding walls; Contracting walls; Magnetohydrodynamics; Nanofluid; Bifurcation diagram; Hermite- Padé approximation

1. Introduction

Nanofluid is a new dynamic subclass of nanotechnology-based heat transfer fluids obtained by dispersing and stably suspended

nanoparticles into base water with typical dimensions of shape and size 1-100nm Choi [1]. MHD Nanofluid flow through porous medium has received attention of many

researchers due to its applications in technological and engineering problems such as MHD generator; plasma studies, nuclear reactors, geothermal energy extraction. Muhammad Zubair Akbar et al. [2] studied heat and mass transfer analysis in a viscous unsteady MHD nanofluid flow through a channel with porous walls and medium in the presence of metallic nanoparticle. Elahi et al. [3] studied theoretical study of blood flow of nanofluid through composite stenosed arteries with permeable walls. The problem of laminar nanofluid flow in a semi-porous channel in the presence of transverse magnetic field was investigated analytically by Sheikholeslami et al. [4]. Their results showed that velocity boundary layer thickness decreases with increases of Reynolds number and it increases as Hartmann number increases. Several studies have been published recently on the modeling of natural convection heat transfer in nanofluids such as [5-7].

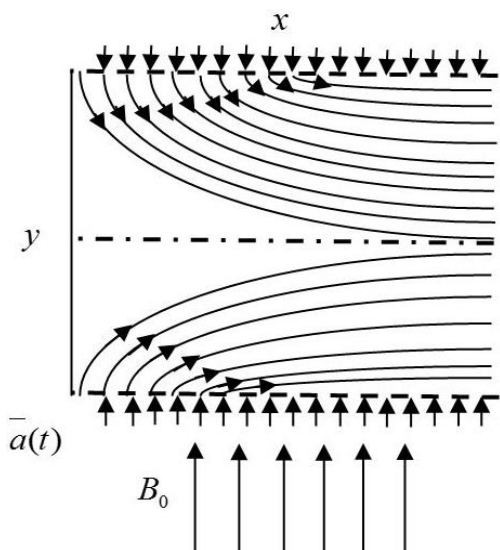
Majdalani et al. [8] studied two dimensional viscous flows between slowly expanding, contracting walls with weak permeability. Seepage across permeable walls is clearly important to the mass transfer between blood, air and tissue [9]. Therefore, a substantial amount of research work has been invested in the study of the flow in rectangular domain bounded by two moving porous walls, which enable the fluid to enter or exit during successive expansions or contractions. Dauenhauer and Majdalani [10] studied the unsteady flow in semi-infinite expanding channels with wall injection. They characterized the two non-dimensional parameters, the expansion ratio of the wall and the cross-flow Reynolds number. Hatami et al. [11] studied numerical analysis of nanofluid flow conveying nanoparticles through expanding and contracting gaps between permeable walls.

The objectives of the present paper are to investigate the influence of magnetic field on nanofluid flow through expanding or contracting channel with permeable walls.

The reduced ordinary differential equations are solved using Hermite-Pade` approximation method. The bifurcation point of wall shear stress and velocity field are obtained due to wall dilation rate and the effects of physical governing parameters on velocity profile are also analysed graphically.

2. Mathematical formulation

Consider the laminar unsteady and incompressible between two porous plates that enable the fluid to enter or exit during successive expansions or contractions shown in Fig. 1. A water based different nanofluids are considered and assumed that the base fluid and the nanoparticles are in thermal



equilibrium and no slip occurs between them. The thermo physical properties of different nanoparticles and base water are given in Table 1.

Fig. 1. Physical configuration of the problem.

Table 1. Thermo physical properties of water and nanoparticles.

Physical properties	Water	Al ₂ O ₃ (Alumina)	Ag (Silver)	Cu (Copper)
$\rho(g/m)$	997.1	3970	10500	8933
$\mu(Pa/s)$	0.001	-	-	-
$\sigma(S/m)$	5.5×10^6	35×10^6	-	59.6×10^6

The walls expand and contract uniformly at a time dependent rate \bar{a} . The fluid inflow velocity is independent of position assumed to be v_w . The continuity and momentum equations for the unsteady flow are as follows.

$$\frac{\partial \bar{u}}{\partial \bar{x}} + \frac{\partial \bar{v}}{\partial \bar{y}} = 0 \quad (2.1)$$

$$\frac{\partial \bar{u}}{\partial \bar{t}} + \bar{u} \frac{\partial \bar{u}}{\partial \bar{x}} + \bar{v} \frac{\partial \bar{u}}{\partial \bar{y}} = -\frac{1}{\rho_{nf}} \frac{\partial \bar{p}}{\partial \bar{x}} + \frac{\mu_{nf}}{\rho_{nf}} \left[\frac{\partial^2 \bar{u}}{\partial \bar{x}^2} + \frac{\partial^2 \bar{u}}{\partial \bar{y}^2} \right] - \frac{\sigma_{nf}}{\rho_{nf}} B_0^2 \bar{u} \quad (2.2)$$

$$\frac{\partial \bar{v}}{\partial \bar{t}} + \bar{u} \frac{\partial \bar{v}}{\partial \bar{x}} + \bar{v} \frac{\partial \bar{v}}{\partial \bar{y}} = -\frac{1}{\rho_{nf}} \frac{\partial \bar{p}}{\partial \bar{y}} + \frac{\mu_{nf}}{\rho_{nf}} \left[\frac{\partial^2 \bar{v}}{\partial \bar{x}^2} + \frac{\partial^2 \bar{v}}{\partial \bar{y}^2} \right] \quad (2.3)$$

where, \bar{u} and \bar{v} are the velocity components in \bar{x} and \bar{y} directions, \bar{p} represents the dimensional pressure, t is the time, B_0 is the magnetic field intensity acting vertically downward on the top plate and $\bar{a}(t)$ is time dependent variable radius.

The boundary conditions are

$$\begin{aligned} \bar{u} = 0, \bar{v} = -V_w = -\frac{\bar{a}}{c} & \quad \text{at} \quad \bar{y} = \bar{a}(t) \\ \frac{\partial \bar{u}}{\partial \bar{x}} = 0, \bar{v} = 0 & \quad \text{at} \quad \bar{y} = 0 \\ \bar{v} = 0 & \quad \text{at} \quad \bar{x} = 0 \end{aligned} \quad (2.4)$$

and $c = \frac{V_w}{a}$ is the injection/suction coefficient.

The dynamic viscosity μ_{nf} , effective density ρ_{nf} and effective electrical conductivity σ_{nf} of the nanofluid are defined by

$$\begin{aligned} \mu_{nf} &= \frac{\mu_f}{(1-\phi)^{2.5}}, \quad \rho_{nf} = (1-\phi)\rho_f + \phi\rho_s, \\ \frac{\sigma_{nf}}{\sigma_f} &= 1 + \left[3 \left(\frac{\sigma_s}{\sigma_f} - 1 \right) \phi / \left(\left(\frac{\sigma_s}{\sigma_f} + 2 \right) - \left(\frac{\sigma_s}{\sigma_f} - 1 \right) \phi \right) \right] \end{aligned} \quad (2.5)$$

Here, ϕ is the solid volume fraction. The stream functions and mean flow vorticity can be written as

$$\begin{aligned} \bar{u} &= \frac{\partial \bar{\psi}}{\partial \bar{y}}, \bar{v} = \frac{\partial \bar{\bar{\psi}}}{\partial \bar{x}}, \bar{\xi} = \frac{\partial \bar{v}}{\partial \bar{x}} - \frac{\partial \bar{u}}{\partial \bar{y}} \\ \frac{\partial \bar{\xi}}{\partial \bar{t}} + \bar{u} \frac{\partial \bar{\xi}}{\partial \bar{x}} + \bar{v} \frac{\partial \bar{\xi}}{\partial \bar{y}} &= \frac{\mu_{nf}}{\rho_{nf}} \left[\frac{\partial^2 \bar{\xi}}{\partial \bar{x}^2} + \frac{\partial^2 \bar{\xi}}{\partial \bar{y}^2} \right] - \frac{\sigma_{nf}}{\rho_{nf}} B_0^2 \frac{\partial \bar{u}}{\partial \bar{y}} \end{aligned} \quad (2.6)$$

Similarity variables are considered due to mass conservation as follows,

$$\begin{aligned} \bar{\psi} &= \frac{\nu_{nf} \bar{x} \bar{f}(y, t)}{a}, \quad \bar{u} = \frac{\nu_{nf} \bar{x} \bar{f}_y}{a^2}, \quad \bar{v} = \frac{-\nu \bar{f}(y, t)}{a}, \\ \bar{y} &= \frac{\bar{y}}{a}, \quad \bar{f}_y = \frac{\partial \bar{f}}{\partial \bar{y}} \end{aligned} \quad (2.7)$$

Substitution Eq. (2.7) into Eq. (2.6) reduces to

$$\bar{u}_{\bar{y}\bar{t}} + \bar{u}\bar{u}_{\bar{y}\bar{x}} + \bar{v}\bar{u}_{\bar{y}\bar{y}} = \nu_{nf} \bar{u}_{\bar{y}\bar{y}\bar{y}} - \frac{\sigma_{nf}}{\rho_{nf}} B_0 \bar{u}_{\bar{y}} \quad (2.8)$$

The chain rule is used to solve Eq. (2.8)

$$\begin{aligned} \bar{f}_{\bar{y}\bar{y}\bar{y}\bar{y}} + \alpha \left(y \bar{f}_{\bar{y}\bar{y}} + 3 \bar{f}_{\bar{y}\bar{y}} \right) + \bar{f} \bar{f}_{\bar{y}\bar{y}} - \bar{f}_{\bar{y}} \bar{f}_{\bar{y}\bar{y}} \\ - a^2 \left(\frac{\mu_{nf}}{\rho_{nf}} \right)^{-1} \bar{f}_{\bar{y}\bar{y}\bar{t}} - a^3 \left(\frac{\sigma_{nf}}{\mu_{nf}} \right) B_0 \bar{f}_{\bar{y}\bar{y}} = 0 \end{aligned} \quad (2.9)$$

With the following boundary conditions

$$\bar{f} = 0, \bar{f}_{\bar{y}\bar{y}} = 0 \quad \text{at} \quad \bar{y} = 0$$

$$\text{and} \quad \bar{f} = \text{Re}' A(1-\phi)^{2.5}, \quad \bar{f}_{\bar{y}} = 0 \quad \text{at} \quad \bar{y} = 1 \quad (2.10)$$

Where $\alpha(t) \equiv \frac{a\bar{a}}{\nu_f}$ is the non-dimensional wall dilation rate which is define positive for expansion and negative for contraction,

$\text{Re}' = \frac{\rho_f a V_w}{\mu_f}$ is the permeation Reynolds number and $\text{Ha}' = B_0 \sqrt{\frac{\sigma_f}{\mu_f}}$ is Hartmann number.

Eq. (2.7), Eq. (2.9) and Eq. (2.10) can be normalized by taking

$$\psi = \frac{\bar{\psi}}{aa}, u = \frac{\bar{u}}{a}, v = \frac{\bar{v}}{a}, f = \frac{\bar{f}}{\text{Re} AB} \quad (2.11)$$

and then

$$\psi = \frac{xf}{c}, u = \frac{xf}{c}, v = \frac{-f}{c}, c = \frac{\alpha}{\text{Re} AB} \quad (2.12)$$

$$f^{iv} + \alpha(yf''' + 3f'') + \text{Re}' AB(f'f'' - ff'') - Ha'^2 C f'' = 0 \quad (2.13)$$

Boundary conditions Eq. (2.10) reduce to

$$y=0: f=0, f''=0$$

$$\text{and } y=1: f=1, f'=0 \quad (2.14)$$

$$A = (1-\phi) + \frac{\rho_s}{\rho_f} \phi, \quad B = (1-\phi)^{2.5},$$

$$C = 1 + \left[3 \left(\frac{\sigma_s}{\sigma_f} - 1 \right) \phi / \left(\left(\frac{\sigma_s}{\sigma_f} + 2 \right) - \left(\frac{\sigma_s}{\sigma_f} - 1 \right) \phi \right) \right]$$

are the constants.

For normalization, substituting $\text{Re} = \frac{\text{Re}'}{\alpha}$ and

$Ha = \frac{Ha'}{\alpha}$ into Eq. (2.15) becomes

$$f^{iv} + \alpha(yf''' + 3f'') + \alpha \text{Re} AB(f'f'' - ff'') - \alpha Ha^2 C f'' = 0 \quad (2.15)$$

2.1 Series Analysis

A power series considered in terms of α in the following form as Eq. (2.15) is nonlinear

$$f(y) = \sum_0^{\infty} f_i \alpha^i \quad (2.16)$$

Substituting the Eq. (2.16) into Eq. (2.15) and equating the coefficient of power series α , with the help of MAPLE, we have computed the first 13 coefficients for the series of the stream function $f(y)$. The first few coefficients of the series of $f(y)$ are as follows.

$$\begin{aligned} f(y, \text{Re}, Ha, A, B, C, \alpha) = & \frac{3}{2} y - \frac{1}{2} y^3 + \left(\frac{1}{140} \text{Re} AB + \frac{1}{10} \right. \\ & - \frac{1}{40} Ha^2 C y + \left(-\frac{1}{5} + \frac{1}{20} Ha^2 C - \frac{3}{280} \text{Re} AB \right) y^3 + \\ & \left(\frac{1}{10} - \frac{1}{40} Ha^2 C \right) y^5 + \frac{1}{280} \text{Re} AB y^7 \alpha + \left(\frac{2}{175} - \frac{17}{2100} Ha^2 C \right. \\ & - \frac{703}{1293600} \text{Re}^2 A^2 B^2 - \frac{37}{4200} \text{Re} AB + \frac{23}{11200} \text{Re} AB Ha^2 C + \\ & \frac{11}{8400} Ha^4 C y + \left(-\frac{13}{350} + \frac{31}{350} Ha^2 C + \frac{73}{107800} \text{Re}^2 A^2 B^2 \right. \\ & + \frac{37}{3150} \text{Re} AB - \frac{23}{8400} \text{Re} AB CHa^2 - \frac{9}{2800} Ha^4 C y^3 + \\ & \left. \left(-\frac{3}{5600} \text{Re} AB CHa^2 - \frac{1}{50} Ha^2 + \frac{3}{1400} \text{Re} AB + \frac{1}{100} Ha^4 C \right. \right. \\ & + \frac{1}{25} y^5 + \left(-\frac{3}{700} \text{Re} AB + \frac{3}{19600} \text{Re}^2 A^2 B^2 - \frac{1}{70} + \right. \\ & \frac{1}{1680} Ha^4 C + \frac{3}{2800} \text{Re} AB CHa^2 \left. \right) y^7 + \left(\frac{-1}{1260} \text{Re} AB \right. \\ & - \frac{1}{3360} \text{Re}^2 A^2 B^2 + \frac{1}{6720} \text{Re} AB CHa^2 \left. \right) y^9 + \\ & \left. \left. \frac{1}{92400} \text{Re}^2 A^2 B^2 y^{11} \right) \alpha^2 + O(\alpha^3) \right) \end{aligned} \quad (2.17)$$

3. Numerical procedure: Hermite-Padé Approximants.

To compute the criticality conditions of the flow, we shall employ a very efficient solution method, known as Hermite-Padé approximants, which was first introduced by Padé [12] and Hermite [13]. We say that a function is an *approximant* for the series

$$S = \sum_{n=0}^{\infty} s_n \alpha^n \quad (3.1)$$

if it shares with S the same first few series coefficients at $|\alpha| < 1$. Thus, the simplest approximants are the partial sums of the series S . When the series converges rapidly, such *polynomial* approximants can provide good approximations of the sum.

Because of the continuation of analytical solution and dominating singularity behavior, the bifurcation study is performed using the partial sum of Eq. (3.2). The dominating behavior of the function $S(\alpha)$ represented by a series Eq. (3.1) may be written as

$$S(\alpha) \sim \begin{cases} B + A \left(1 - \frac{\alpha}{\alpha_c}\right)^\delta & \text{when } \delta \neq 0, 1, 2, \dots, \\ B + A \left(1 - \frac{\alpha}{\alpha_c}\right)^\delta \ln \left|1 - \frac{\alpha}{\alpha_c}\right| & \text{when } \delta = 0, 1, 2, \dots \end{cases} \quad (3.2)$$

As $\alpha \rightarrow \alpha_c$, where A and B are some constants and α_c is the critical point with the critical exponent δ .

Assume that the $(d+1)$ tuple of polynomials, where d is a positive integer:

$$P_N^{[0]}, P_N^{[1]}, \dots, P_N^{[d]}$$

where,

$$\deg P_N^{[0]} + \deg P_N^{[1]} + \dots + \deg P_N^{[d]} + d = N, \quad (3.3)$$

is a Hermite-Padé form of these series if

$$\sum_{i=0}^d P_N^{[i]}(\alpha) S_i(\alpha) = O(\alpha^N) \text{ as } |\alpha| < 1 \quad (3.4)$$

Here $S_0(\alpha), S_1(\alpha), \dots, S_d(\alpha)$ may be independent series or different form of a unique series. We need to find the polynomials $P_N^{[i]}$ that satisfy the Eq. (3.3) and Eq. (3.4). These polynomials are completely determined by their coefficients. So, the total number of unknowns in Eq. (3.4) is

$$\sum_{i=0}^d \deg P_N^{[i]} + d + 1 = N + 1 \quad (3.5)$$

Expanding the left hand side of Eq. (3.4) in powers of α and equating the first N equations of the system equal to zero, we get a system of linear homogeneous equations. To calculate the coefficients of the Hermite-Padé polynomials it requires some sort of normalization, such as

$$P_N^{[i]}(0) = 1 \text{ for some integer } 0 \leq i \leq d \quad (3.6)$$

It is important to emphasize that the only input required for the calculation of the Hermite-Padé polynomials are the first N

coefficients of the series $S_0(\alpha), S_1(\alpha), \dots, S_d(\alpha)$. The Eq. (3.5) simply ensures that the coefficient matrix associated with the system is square. One way to construct the Hermite-Padé polynomials is to solve the system of linear equations by any standard method such as Gaussian elimination or Gauss-Jordan elimination. In practice, one usually finds that the dominant singularities as well as the possibility of multiple solution branches for the nonlinear problem are located at zeroes of the leading polynomial coefficients $P_N^{[d]}(\alpha)$ of the Eq. (3.4). If the singularity is of algebraic type, then the exponent δ may be approximated by

$$\delta_N = d - 2 - \frac{P_N^{[d-1]}(\alpha_{c,N})}{D P_N^{[d]}(\alpha_{c,N})}. \quad (3.7)$$

Drazin-Tourigney Approximants [14] is a particular kind of algebraic approximants and Khan [15] introduced High-order differential approximant (HODA) as a special type of differential approximants.

4. Results and Discussion

By differentiating series Eq. (2.17), we have computed the velocity function f' as a series in power α , Re and Ha respectively. The objective of the present study is to apply Hermite-Padé approximation method to obtain an explicit solution of laminar unsteady incompressible different nanofluid in a parallel channel bounded by two moving porous walls, which enable the nanofluid to enter or exit due to successive expansion or contractions.

Fig. 2 shows the effect of nanoparticles volume fraction on stream function and velocity profiles. As nanoparticles volume fraction increases, fluid velocity $f'(y)$ also increases while the stream function $f(y)$

decreases. It can be seen from Fig. 3 that fluid centerline velocity reduces while increases near the two walls by the decreasing values of permeation Reynolds number Re . It is also shown that in absence of Hartmann number stream function $f(y)$ increases slightly while velocity $f'(y)$ increases sharply. Fig. 4 shows the effect of non-dimensional wall dilation rate α on stream function and fluid velocity. The fluid velocity increases along the centerline with the positively increasing values of dimensionless wall dilation rate due to successive expansion of channel width. On the other hand, velocity decreases at the centre of the channel whereas increases near the two plates when α decreases negatively. The magnetic field has a significant effect on the velocity profile with the variation of α . The

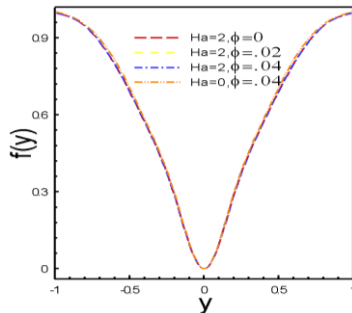


Fig. 2. Effect of Cu-nanoparticles volume fraction on $f(y)$ and $f'(y)$ when $Re = 4, \alpha = 1$.

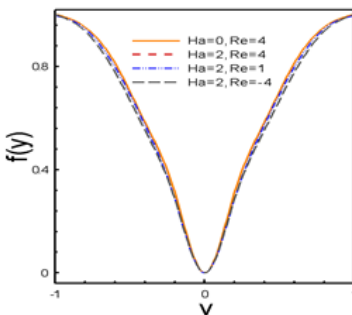


Fig. 2. Effect of Cu-nanoparticles volume fraction on $f(y)$ and $f'(y)$ when $Re = 4, \alpha = 1$.

effect of different nanoparticles volume fraction on $f(y)$ and $f'(y)$ are noticed in Fig. 5. It shows that the Ag-nanoparticles produce larger horizontal velocity near the walls. Moreover, Cu-nanoparticles enhance centerline velocity in absence of magnetic field.

Fig. 6 demonstrates the effect of Hartmann number on stream function and velocity profiles. It is seen that velocity at the centre of the channel reduces while enhances around the two plates when Ha increases. The transverse magnetic field opposes the alteration phenomena clearly. Because the variation of Ha leads to the variation of the Lorentz force due to magnetic field and the Lorentz force produces more resistance to the alteration phenomena.

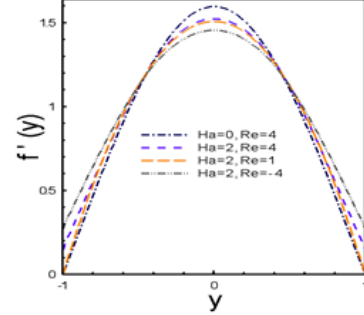
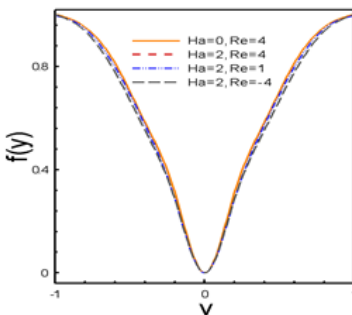
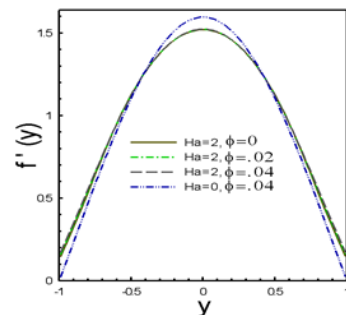


Fig. 3. Effect of Reynolds number on $f(y)$ and $f'(y)$ for Cu-water nanofluid with $\phi = 0.04$ when $\alpha = 1$.

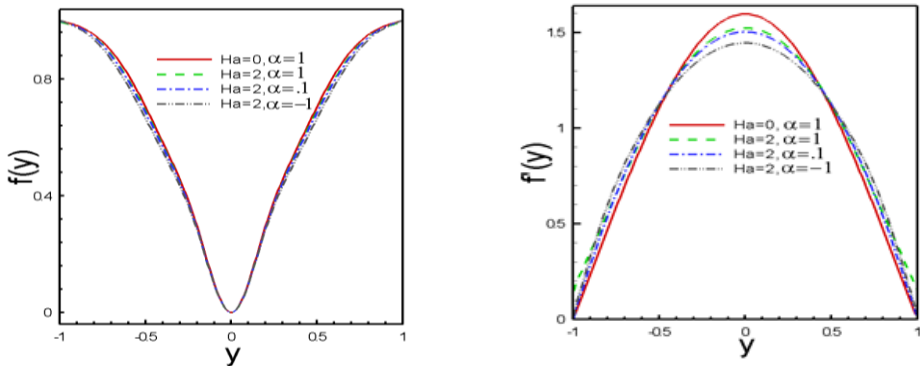


Fig. 4. Effect of non-dimensional wall dilation rate on $f(y)$ and $f'(y)$ for Cu-water nanofluid with $\phi = 0.04$ when $Re = 4$.

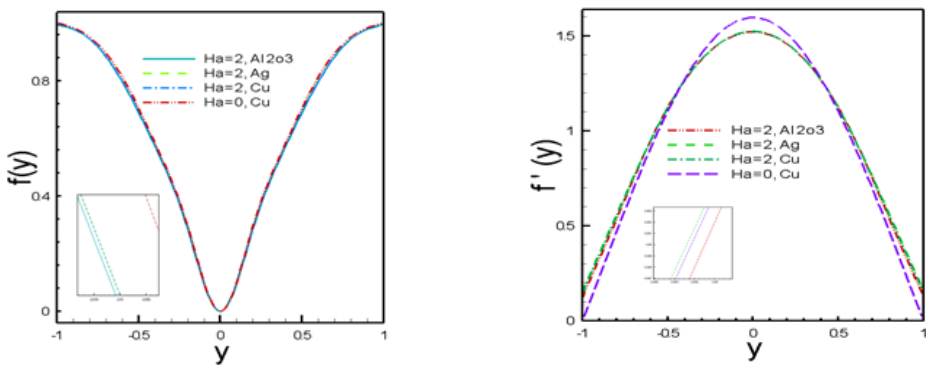


Fig. 5. Effect of different nanoparticles on $f(y)$ and $f'(y)$ for water as base fluid with $\phi = 0.04$ when $Re = 4, \alpha = 1$

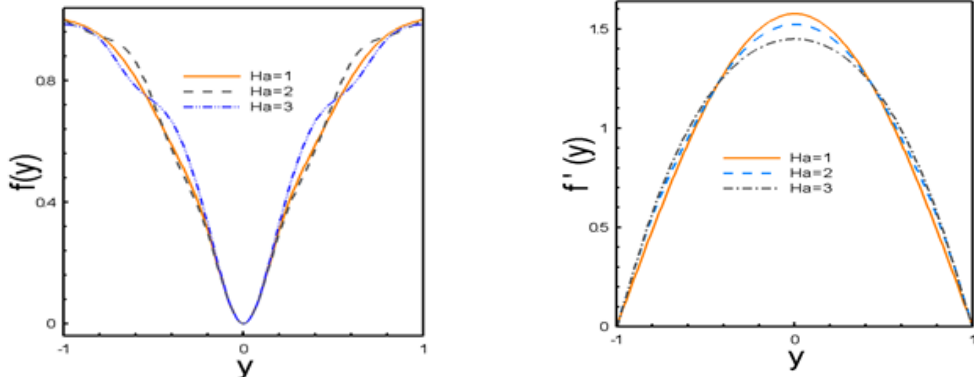


Fig. 6. Effect of Hartmann number on $f(y)$ and $f'(y)$ for Cu-water based nanofluid with $\phi = 0.04$ when $Re = 4, \alpha = 1$

The wall shear stress for different values of permeation Reynolds number over a range of non-dimensional wall dilation rate and Hartmann number are depicted in Fig. 7 (a). The absolute value of shear stress

decreases when Reynolds number is positive as well as the non-dimensional wall dilation rate increases. Moreover, it is also noticed that the wall shear stress decreases rapidly by the positive variation of Ha .

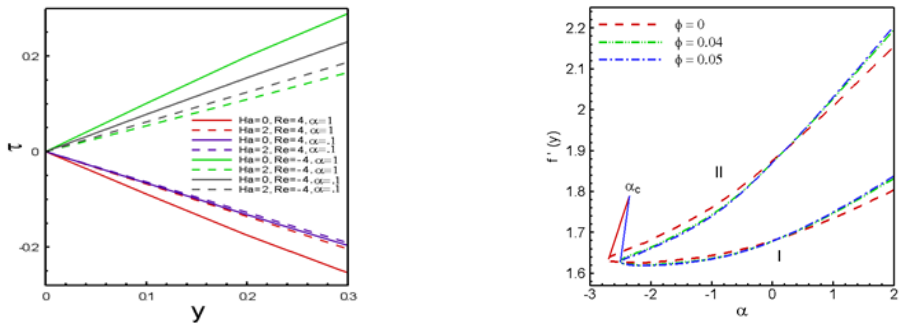


Fig. 7. (a) Dual solution of non-dimensional Shear stress and (b) bifurcation diagram of velocity at the porous wall for Cu-water nanofluid.

Employing the algebraic approximation method to the series Eq. (2.17) we have obtained the dominating singularity behavior of the function $f(y) \approx (\alpha - \alpha_c)^{\frac{1}{2}}$ with $\alpha_c \approx -2.752214$. Fig. 7(b) shows the bifurcation diagram of velocity versus α with the effect of Cu-water nanofluid. We say that there is a *simple turning point, fold or a saddle-node bifurcation* at $\alpha = \alpha_c$. It is interesting to notice that there are two solution branches of velocity when $\alpha > \alpha_c$, one marginal solution when $\alpha = \alpha_c$ and no solution when $\alpha < \alpha_c$, where α_c is the critical value of α for which the solution exists. The stability analysis indicates that the lower solution branch (I) is stable and physically realizable. For different values of ϕ , the upper solution branch (II) is unstable and physically unacceptable shown in Fig. 7(b).

5. Conclusion

The stability of MHD unsteady nanofluids flow through expanding or contracting channel with porous wall in presence of an external magnetic field has been studied numerically. The effects of Hartman number, permeation Reynolds number, non-dimensional wall dilation rate

and nanoparticles volume fraction on velocity profile, stream function and shear stress are investigated numerically. The major results of the current study are given as follows.

- As nanoparticles volume fraction increases velocity profile increases while stream function decreases with presence of Hartmann number.
- The velocity function and stream function also increases by the increasing values of permeation Reynolds number.
- Ag- nanoparticles accelerate horizontal velocity near the walls whereas Cu-nanoparticles enhance centerline velocity.
- The wall shear stress decreases swiftly by the positive variation of Hartmann number.

The fluid velocity at the wall has two branches bifurcating at the critical wall dilation rate at $\alpha = \alpha_c$ namely an upper branch and a lower branch. It is found that at the lower solution branch which is physically acceptable, the value of velocity enhances with the increase in the nanoparticles volume fraction.

References

[1] DAS SK, Choi SUS, Yu W, Pradeep T. Nanofluids: Science and Technology. New York: Wiley; 2007.

[2] Akbar MZ, Ashraf M, Iqbal MF, Ali K. Heat and mass transfer analysis in a viscous unsteady MHD nanofluid flow through a channel with porous walls and medium. *AIP Advances* 2016;6: 45-222. doi: 10.1063/1.4945440.

[3] Elahi R, Rahman SU, Nadeem S, Akbar NS. Blood flow of nanofluid through an artery with composite stenosis and permeable walls. *Appl Nanosci* 2014;4:919-26.

[4] Hatami M, Sheikholeslami M, Ganji DD. Laminar flow and heat transfer of nanofluid between contracting and rotating disks by least square method. *Powder Tech* 2014;253:769-79.

[5] Sheikholeslami M, Hatami M, Ganji DD. Analytical investigation of MHD nanofluid in Semi porous channel. *Powder Tech* 2013;246:327-36.

[6] Sheikholeslami M, Ganji DD. Heat transfer of Cu- water nanofluid flow between parallel plates. *Powder Tech* 2013;235:873-9.

[7] Sheikholeslami M, Hatami M, Ganji DD. Nanofluid flow and heat transfer in a rotating system in the presence of magnetic field. *Journal of Molecular Liquids* 2014;190:112-20.

[8] Majdalani J, Zhou C, Dawson CA. Two-dimensional viscous flow between slowly expanding, contracting walls with weak permeability. *J Biomech* 2002;35: 1399-403.

[9] Chang HN, Ha JS, Park JK, Kim IH, Shin HD. Velocity field of pulsatile flow in a porous tube. *J Biomech* 1989;22:1257-67.

[10] Dauenhuer EC, Majdalani J. Unsteady flows in semi-infinite expanding channels with wall injection. *AIAA paper* 1999:99-3523.

[11] Hatami M, Sahebi SAR, Majidian A, Sheikholeslami M, Jing D, Domairry G. Numerical analysis of nanofluid flow conveying nanoparticles through expanding and contracting gaps between permeable walls. *J Mol Liq* 2015;212:785-91.

[12] Padé H. Sur la représentation approchée d'une fonction pour des fractions rationnelles. *Ann Sci École Norm* 1892;9:1-93.

[13] Hermite C. Sur la généralisation des fractions continues algébriques: *Annali di Mathematica Pura e Applicata*. 1893;21(2):289-308.

[14] Drazin PG, Tourigny Y. Numerically study of bifurcation by analytic continuation of a function defined by a power series. *SIAM Journal of Applied Mathematics* 1996;56:1-18.

[15] Khan MAH. High- Order Differential Approximants. *J Comp Appl Math* 2002;149:452-68.